# Technical Memorandum

**To:** Jeff Uhlmeyer

**From:** Gary Elkins, Lauren Gardner, Gonzalo Rada and Kevin Senn

**cc:** Mustafa Mohamedali

**Date:** April 7, 2020 (original)

**Re.** Forensic Desktop Study Report: Oklahoma LTPP Test Sections 40_AA**

The Long-Term Pavement Performance (LTPP) Specific Pavement Studies (SPS) test sections 40_AA01, 40_AA02, 40_AA03, 40_AA61, 40_AA62, and 40_AA63[1] were nominated for a desktop study under TPF-5(332) "LTPP Forensic Evaluations." The study is focused on investigating the reason cracking, specifically non-wheel path longitudinal cracking, re-appeared a year after a 2-inch Warm Mix Asphalt (WMA) overlay was applied to the test sections. The proposed investigation is intended to determine if the cracks that re-appeared following the overlay are reflection cracks, to capture the time before crack initiation, and to compare the performance to date for the Oklahoma SPS-10 test sections.

## SITE DESCRIPTION

LTPP test sections 40_AA01, 40_AA02, 40_AA03, 40_AA61, 40_AA62, and 40_AA63 are located on State Route 66, westbound, in Canadian County, Oklahoma. State Route 66 is an urban principal arterial with two lanes in the direction of traffic. It is classified as being in a Wet, No Freeze climate zone with an average annual precipitation ranging between 29.5 inches (2016) and 57.7 inches (2015). The test sections have an annual average air freezing index ranging between 70.2 deg-F deg-days (2016) and 133.2 deg-F deg-days (2015) during the performance period in question (2015 to 2018). The coordinates of the test sections are provided in Table 1. Attachment A includes photographs of test sections 40_AA01, 40_AA02, 40_AA03, 40_AA61, 40_AA62, and 40_AA63 at Station 0+00 looking westbound in 2017, while Map 1 shows the geographic location of the test sections relative to Oklahoma City, Oklahoma. In total, the test sections span approximately 1.8 miles of roadway; Figure 1 shows the project design layout.

[1] First two digits represent the State Code [40 = Oklahoma]. The next characters after the underscore represents the project number (A for first project, B for second project, etc.), while the character that follows is always "A," which denotes the SPS-10 experiment. There is only one SPS-10 project site in Oklahoma. The third and fourth characters that follow are for the project and section numbers – e.g., 40_AA01 represents the core test section 01 within the SPS-10 project in the State of Oklahoma, 40_AA02 represents core test section 02, and 40_AA61 represents the state supplemental test section 61 within the same project. Figure 1 presents details of the test section at this project site.

Wood Environment & Infrastructure Solutions, Inc.
12000 Indian Creek Ct, Suite F
Beltsville, MD 20705
+1 301-210-5105
www.woodplc.com

**Table 1. Coordinates of test section locations.**

| Test Section | Latitude | Longitude |
|---|---|---|
| 40_AA01 | 35.50806 | -97.79262 |
| 40_AA02 | 35.50802 | -97.79927 |
| 40_AA03 | 35.50798 | -97.80479 |
| 40_AA61 | 35.508 | -97.80959 |
| 40_AA62 | 35.508 | -97.81493 |
| 40_AA63 | 35.50797 | -97.82235 |


**Map 1. Geographical location of test section relative to Oklahoma City, Oklahoma.**

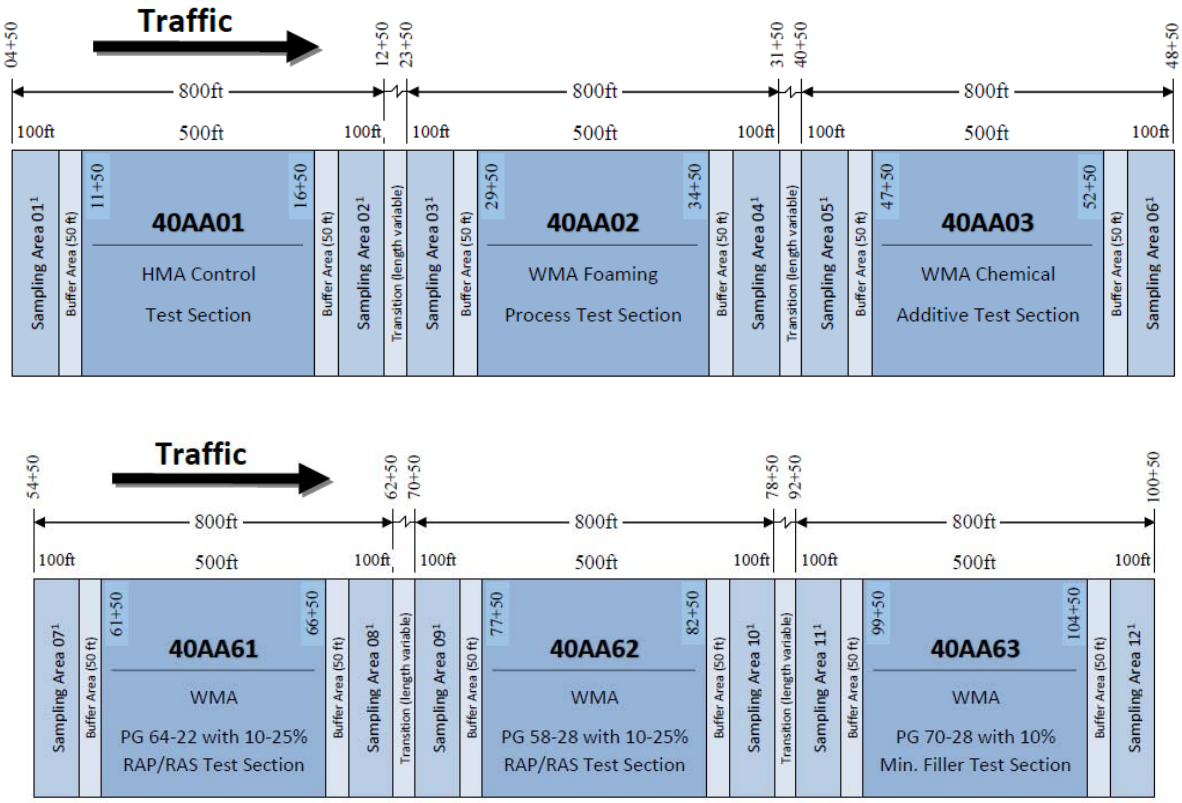


**Figure 1. Project design layout.**

# BASELINE PAVEMENT HISTORY

This section of the document presents historical data on the pavement structure and its structural capacity, climate, traffic and pavement distresses.

## Pavement Structure and Construction History

The six Oklahoma test sections were incorporated into the LTPP program in March 2015 as part of the SPS-10 Warm Mix Asphalt Experiment. The pavement at these test sections was originally constructed in the late 1930's and was reconstructed in the 1960s. While several maintenance and rehabilitation activities (which were not well documented) occurred after the 1960s reconstruction, the pavement structure at the time of its inclusion into the LTPP program in 2015 is considered the original pavement structure, and consisted of approximately 10 inches of Asphalt Concrete (AC) on 12 inches of a soil aggregate mixture over a fine grained (clay) subgrade. The pavement structures for each test section at the time they were incorporated into the LTPP program are summarized in Table 2; this information corresponds to CONSTRUCTION_NO = 1 (CN = 1) in the LTPP database. As the table shows, the total AC thicknesses for the sections varied between 8.8 and 10.8 inches, was composed of 5 identified dense graded HMAC layers, and, as will be repeated throughout this memorandum, the AC thickness was intended to be uniform throughout the test sections, thus the variation in thickness was not part of the experiment design. The table also shows that the thickness of the soil aggregate mixture is 12.0 inches for all test sections; i.e., it is the same for all test sections to a tenth of an inch, which is highly unlikely, but it represents the information contained in the LTPP database – clarification will need to be pursued further as part of the follow-up investigations.

.

**Table 2. Pavement structure for CN = 1.**

| Layer Number | Layer Type | Material Description | Thickness (in.) for Section 40_AA** | | | | | |
|---|---|---|---|---|---|---|---|---|
| | | | 01 | 02 | 03 | 61 | 62 | 63 |
| 1 | Subgrade (untreated) | Fine-Grained Soils: Clay | Assumed semi-infinite for layer moduli backcalculation purposes | | | | | |
| 2 | Unbound (granular) base | Soil-Aggregate Mixture (Predominantly Fine-Grained) | 12.0 | 12.0 | 12.0 | 12.0 | 12.0 | 12.0 |
| 3 to 7 | Asphalt concrete layer | Hot Mixed, Hot Laid AC, Dense Graded | 8.8 | 10.4 | 9.7 | 10.1 | 10.5 | 10.8 |

A second construction event took place in November 2015 (CN = 2), when the AC surface layer of each test section was milled and then received a 2-inch AC overlay. Per the experiment design, the type of asphalt mix varied from section to section. Table 3 summarizes the differences in mixes used for the AC overlay at each of the test sections. As described in Table 3 as well as below, test section 40_AA01 was the control section and received a conventional hot-mix asphalt (HMA) overlay, sections 40_AA02, 40_AA03, 40_AA61, and 40_AA62 received WMA overlays, and section 40_AA63 received a stone-matrix asphalt (SMA) overlay. Besides differences in type of asphalt mix used, the following bullet items provide additional information for each test section:

- *Section 40_AA01*: Because an HMA overlay was used at this test section, both the mix and compaction temperatures of the overlay were higher than those of the other asphalt mixtures. After milling and placement of the WMA overlay, it had a total AC layer combined thickness of 9.4 inches, and was the thinnest test section at this site. It is noted the thickness of the AC layers were intended to be uniform throughout the test sections, and the variation in thickness was not part of the experiment design
- *Section 40_AA02*: This WMA foam overlay test section is the first of four WMA test sections. For this test section and the remaining three WMA test sections, a chemical package that included cationic emulsification agents, anti-stripping agents, and additives to enhance aggregate coating and workability was used. Mix and laydown temperature conditions at the time of mixing and compaction were the same or similar to the other three WMA asphalt mixes. It has an asphalt layer combined thickness of 11.0 inches after placement of the overlay.
- *Section 40_AA03*: This WMA chemical additive overlay test section is the second of four WMA test sections. Mix and laydown temperature conditions at the time of mixing and compaction were the same or similar to the other three WMA asphalt mixes. It has an asphalt layer combined thickness of 10.3 inches.
- *Section 40_AA61*: This WMA chemical additive, reduced grade asphalt, and recycled asphalt pavement and shingles (RAP and RAS) overlay test section is the third of four WMA test sections and the first of three state supplemental test sections. Mix and laydown temperature conditions at the time of mixing and compaction were the same or similar to the other three WMA asphalt mixes. It has an asphalt layer combined thickness of 10.4 inches.
- *Section 40_AA62*: This WMA chemical additive and reduced grade asphalt overlay test section is the last of four WMA test sections and the second of three state supplemental test sections. Mix and laydown temperature conditions at the time of mixing and compaction were the same or like the other three WMA asphalt mixes. It has an asphalt layer combined thickness of 10.6 inches.

- *Section 40_AA63*: This is a Stone Matrix Asphalt (SMA) overlay supplemental test section. For this test section a chemical package that included cationic emulsification agents, anti-stripping agents, and additives to enhance aggregate coating and workability was used. Mix and laydown temperature at the time of mixing and compaction were the same or similar to those of the WMA asphalt mixes, but the binder content was significantly higher—6.6%. It has an asphalt layer combined thickness of 10.8 inches.

**Table 3. Pavement mix summary.**

| Mix 1 | Mix 2 | Mix 3 | Mix 4 | Mix 5 | Mix 6 |
|---|---|---|---|---|---|
| 40AA01 | 40AA02 | 40AA03 | 40AA61 | 40AA62 | 40AA63 |
| HMA Control | WMA Foam | WMA Chemical | WMA Chemical + PG Drop + RA | WMA Chemical + 2 × PG Drop | SMA Chemical |
| 70-28 | 70-28 | 70-28 | 64-22 | 58-28 | 70-28 |
| NA | 2.0 | 0.7 | 0.7 | 0.7 | 1.0 |
| 3.7 | 3.7 | 3.8 | 3.8 | 3.8 | 6.6 |
| 4.9 | 4.9 | 5.0 | 5.0 | 5.0 | 6.6 |
| 163 | 135 | 141 | 141 | 141 | 141 |
| 152 | 127 | 129 | 129 | 129 | 129 |
| 12 | 12 | 12 | 12 | 12 | NA |
| 3 | 3 | 3 | 3 | 3 | NA |

The final pavement structure of each test section, after mill and overlay, is summarized in Table 4.

**Table 4. Pavement structure after mill and experimental overlay placement (CN = 2).**

| Layer Number | Layer Type | Material Description | Thickness (in.) for Section 40_AA** | | | | | |
|---|---|---|---|---|---|---|---|---|
| | | | 01 | 02 | 03 | 61 | 62 | 63 |
| 1 | Subgrade (untreated) | Fine-Grained Soils: Clay | Assumed semi-infinite for layer moduli backcalculation purposes | | | | | |
| 2 | Unbound (granular) base | Soil-Aggregate Mixture (Predominantly Fine-Grained) | 12.0 | 12.0 | 12.0 | 12.0 | 12.0 | 12.0 |
| 3 to 8 | Asphalt concrete layer | All bituminous concrete layers | 9.4 | 11.0 | 10.3 | 10.4 | 10.6 | 10.8 |

## Pavement Structural Deflection Response Properties

Figure 2 shows the average Falling Weight Deflectometer (FWD) deflection under the nominal 9,000-pound load plate over time for each test section. The deflection of the sensor located in the center of the load plate is a general indication of the total "strength" or response of all layers in the pavement structure to a vertically applied load. This deflection can be influenced by pavement temperature at the time of testing, and changes in in-situ moisture in the unbound layers, and pavement structure over time.

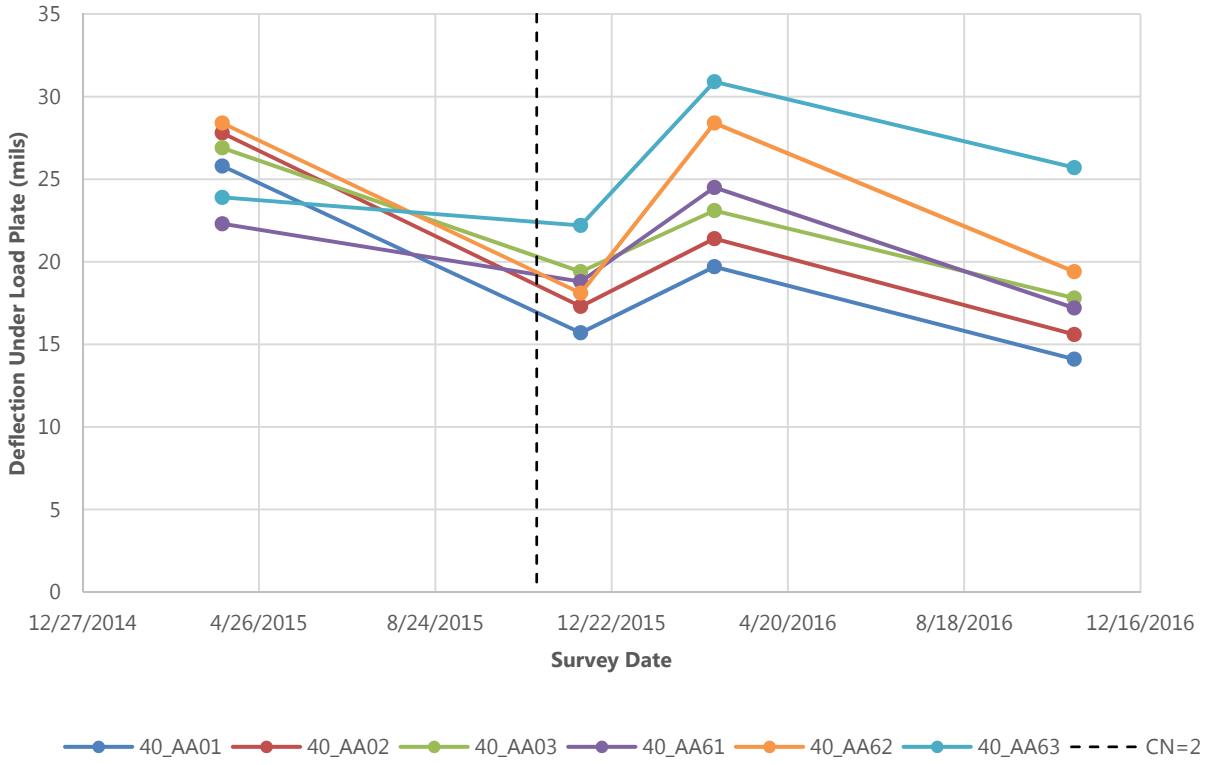


**Figure 2. Average deflection for the sensor located in the load plate normalized to 9,000 lb. drop load over time.**

The pavement structures of the test sections, prior to the treatment of the sections with the AC overlay in November of 2015, reported similar deflections; the initial reported deflections ranged from 22.3 mils (for Section 40_AA61) to 28.4 mils (for Section 40_AA62). As expected, following the application of the AC

overlay, the deflections observed for each of the test sections decreased as the AC overlay provided additional structural capacity to the pavement. Section 40_AA01 reported the lowest levels of deflection after the AC overlay was applied, 15.7 mils, while Section 40_AA63 reported the highest deflections of the test sections, 22.2 mils. These results appear to directly related to the total thickness of the AC layers – as shown in Table 4, the total AC thickness for Section 40_AA01 is 9.4 inches (lowest value), while the total AC thickness for Section 40_AA63 is 10.8 inches (second highest value) and for Section 40_AA02 is 11.0 (highest value and second lowest deflection after Section AA_AA01). The deflections observed for each of the test sections increased by November 2016 with the SMA overlay exhibiting the highest deflections of the test sections and the HMA overlay reporting the lowest. The deflections observed ranged between 14.1 mils (Section 40_AA01) and 25.7 mils (Section 40_AA63).

In addition to the deflection variations due to the overlay type, the deflections also varied due to temperature. The months where higher deflections were reported correspond to months with warmer weather—April 2015 and March 2016. The average air temperature reported at the time of testing for April 2015 and March 2016 was 76.5 Deg F and 68.0 Deg F, respectively. The two months where lower deflections were reported correspond to months with colder weather. The average air temperature at the time of testing in December 2015 and November 2016 was 60.0 Deg F and 55.7 Deg F, respectively. Overall, when overlay type and temperature is considered, the measured deflections for each of the test sections appear to be reasonable.

## Climate History

The historical annual average precipitation for the test sections is depicted in Figure 3. Despite the test sections being collocated along a 1.8 mile section, the annual average precipitation was reported for two groups of test sections; one group consisted of sections 40_AA01, 40_AA02, 40_AA03, and 40_AA61 while the second group consisted of sections 40_AA61 and 40_AA63. Therefore, an average of these two groups is reported in Figure 3. In 2015, the average amount of precipitation reported was a maximum of 54.5 inches—which is nearly 60 percent more than the amount of precipitation observed in 2016. The minimum annual average precipitation was reported in 2016 at 32.1 inches.

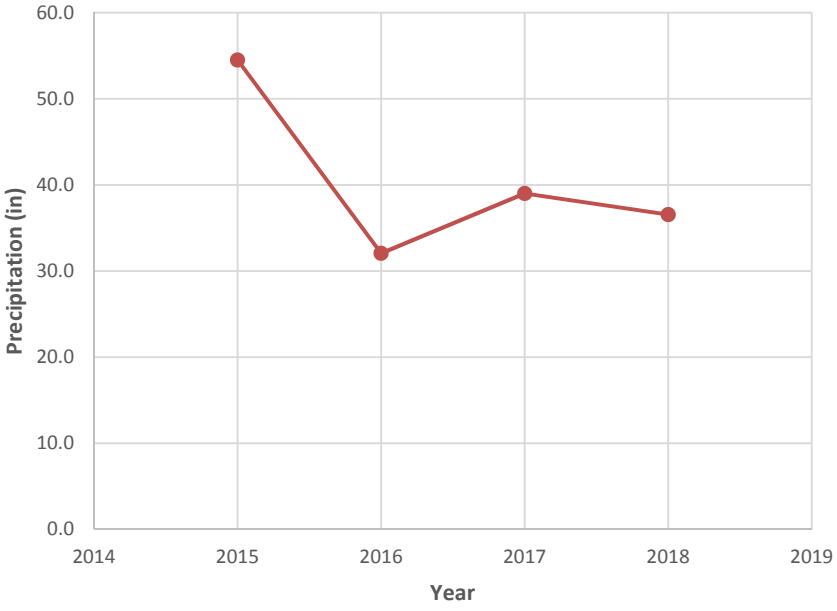


**Figure 3. Average annual precipitation over time.**

Figure 4 shows the time history of the average annual freezing index for the test sections. Again, despite the test sections being collocated along a 1.8 mile section, the average annual freezing index was also reported for the same two groups of test sections as for precipitation; i.e., one group consisted of sections 40_AA01, 40_AA02, 40_AA03, and 40_AA61, while the second group consisted of sections 40_AA61 and 40_AA63. This means that this location is at the boundary between two Modern Era Retrospective-Analysis for Research and Applications (MERRA) cells that are approximate 43 miles wide by 30 miles tall. An annual average of these two MERRA cells is reported in Figure 4. The freezing index is the sum of the difference between 32 degrees F and the average air temperature when it is less than freezing and 32 degrees F for each day, which is summed over a year's time. This index is an indicator of the harshness of the winter season relative to issues such as ground frost and low temperature cracking in pavements. As shown in Figure 4, the freezing index values ranged from 72 deg F deg days (in 2016) to 132.3 deg F deg days (in 2015). The annual freezing indices reported are considered moderate to approaching the classification as a freeze zone. An average annual freezing index over 150 deg F days is classified by LTPP as a freeze zone.

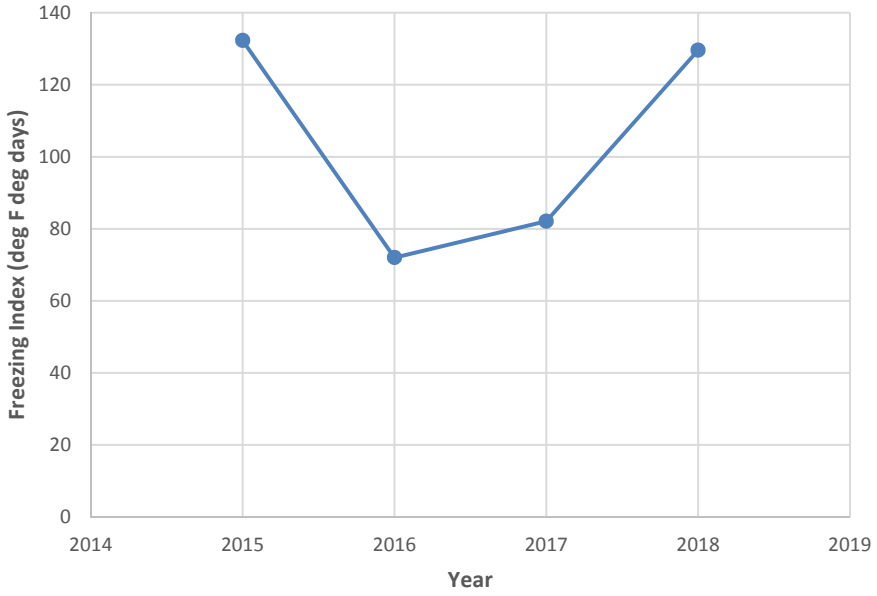


**Figure 4. Average annual air temperature freezing index over time.**

This project site is in a climate that experiences a large number of freeze thaw cycles every year. It has been postulated that this zone can be more damaging to a pavement since the unbound layers can go through more freeze thaw cycles in a year than in deep freeze areas, where the unbound materials freeze once and thaw out once in each winter cycle. Figure 5 shows the annual umber of air temperature freeze-thaws days. A freeze thaw day is where the maximum air temperature day is greater than 32 deg F and the minimum air temperature is less than 32 deg F on each day, summed up for the calendar year. A value of 90 indicates that within a year, there was roughly the equivalent of three months where the air temperature air transitioned the freezing point of water. The time history for this parameter starts in 1988 to provide a broader time scale since the existing pavement structure temperature was subjected to these patterns. It is interesting that since placement of the overlays in 2015, the number of freeze thaw cycles was very low and reached a minimum value in 2017.

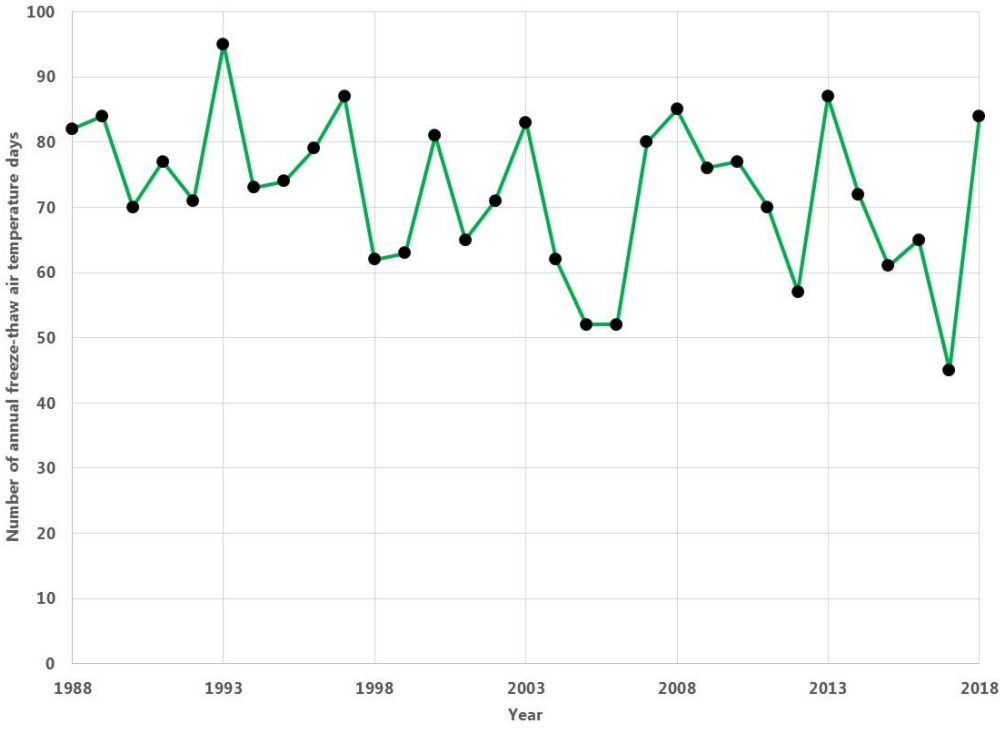


**Figure 5. Annual days of air temperature freeze thaw cycles.**

## Truck Volume History

A weight-in-motion (WIM) was installed at the Oklahoma SPS-10 in 2016. Figure 6 shows the annual average daily truck traffic (AADTT) data in the LTPP test lane for all sections by year. Based on the figure, the test sections received an increase in truck traffic over time. In 2016, or the year after the overlay was applied, the AADTT was reported as 183 on the test sections. The AADTT reported in 2017 and 2018 increased to 236 and 308, respectively. By 2019, 305 trucks per day were observed on the six test sections, which represents an approximately 60% increase in truck traffic over a three-year period and which is significant and could have impacted on the performance of the pavement test sections.

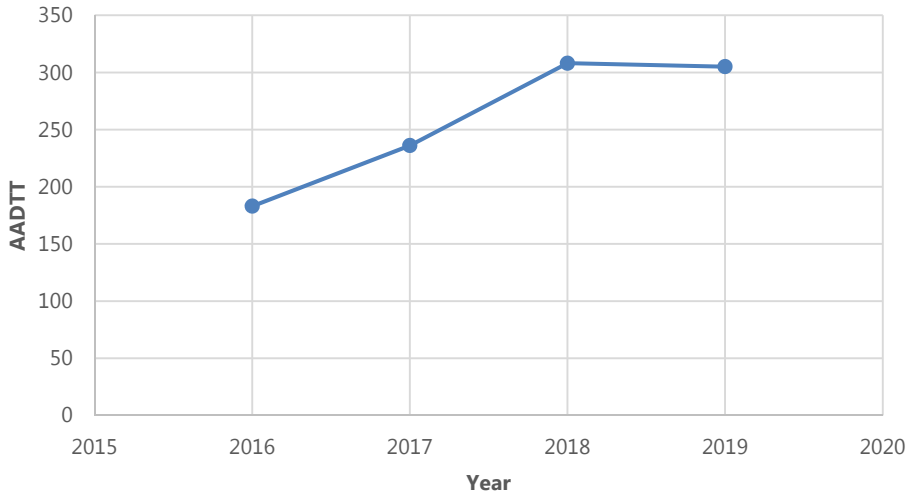


**Figure 6. Average annual daily truck traffic (AADTT) history.**

## Pavement Distress History

The following section summarizes the distresses observed on the test section between the time the section was constructed and 2019, which is when the last manual distress survey was performed on the test sections. Fatigue cracking, longitudinal cracking (off the wheel path), transverse cracking, edge cracking, block cracking, IRI, and rutting were assessed. No patching was observed following the overlay.

### Fatigue Cracking

Figure 7 summarizes the total area in which fatigue/alligator cracking was observed prior to and after the application of the AC overlay in November 2015. As shown in the figure, fatigue cracking prior to the overlay varied by section. Section 40_AA62 exhibited the most cracking, 2,279.8 square feet or approximately 38% of the test section's area, and section 40_AA03 exhibited the least amount of fatigue/alligator cracking, 255.1 square feet or approximately 4% of the test section prior to the overlay.

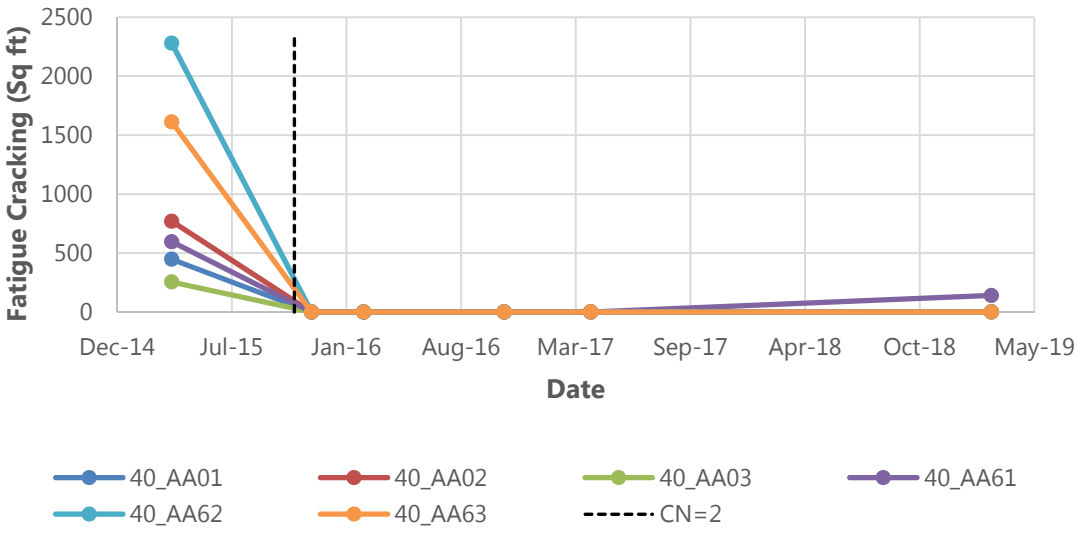


**Figure 7. Time history of the area of fatigue/alligator cracks.**

Figure 8 shows the fatigue/alligator cracking on test section 40_AA62 prior to placement of the overlay. Note that the severe cracking on the inside portion of the lane appears to be outside the wheel path. In Figure 9 shows an after overlay image of this test section where it is easier to actual wheel path locations. The longitudinal crack down the outside portion of the lane was also rated as fatigue/alligator cracking. It is interesting that the most severe cracks are at the outside wheel path edges where shear stresses tend to be the greatest. The transverse cracks seen in this figure were rated as block cracking, however some of these cracks could also have been rated as transverse cracks.

While the fatigue/alligator cracking reported prior to the overlay varied greatly between sections (potentially due to variations in total AC thickness), no fatigue cracking was observed on any of the test sections between 2015 and March 2017 following the AC overlay. By March 2019, there were three sections where fatigue cracking was observed: section 40AA01 with 1.1 $ft^2$, section 40_AA02 with 1.1 $ft^2$, and section 40_AA61 with 139.9 $ft^2$. These sections represent the HMA overlay and two WMA overlays of varying thicknesses. They do not represent the sections with highest amounts of fatigue cracking observed prior to the overlay. Figure 10 is an image of section 40_AA62 from March 2019 at the same location as Figure 8. While this test section had the greatest amount of cracking prior to the overlay, in 2019 it the longitudinal crack between lanes had reappeared and a minor amount of longitudinal on the outside edge of the lane had started to appear on the pavement surface. The chalk marks indicate where the data collection contractor thought the middle of the right wheelpath and lane center were located.


**Figure 8. Image of section 40_AA62 in April 2015 at station 0+00 prior to overlay showing severe level of cracking. This test section was rated as having block cracking and no transverse cracking.**

**Figure 9. Image of test section 40_AA62 in March 2019 at station 0+00 approximately 3.5 years after mill and overlay. The longitudinal chalk lines show lane center and middle of right wheel path, where the line of FWD measurements will be performed along the test section.**

Moreover, because cracking is now starting to reappear on the surface of some test sections which previously had some severe cracking patterns, it is important to continue to monitor this cracking in order to enable better quantification or modeling of crack initiation and crack propagation.

## Longitudinal Cracking

No longitudinal cracking has been observed in the wheel paths (WP) since 2015, so this desktop study only considers non-wheel path (NWP) longitudinal cracking.

Figure 10 depicts the NWP longitudinal cracking observed from 2015 to 2019. Looking at this distress feature alone can lead to faulty conclusions. While sections 62 and 63 had very low rated NWP longitudinal cracking prior to overlay, judging by Figure 8, section 62 had many other types of cracking that were longitudinal in nature, not located in the wheel path, but appear to have been rated in other distress categories. Looking at figure 9, there is a very straight NWP longitudinal crack between the lanes, when such a crack did not exit prior to the overlay as shown in figure 8.

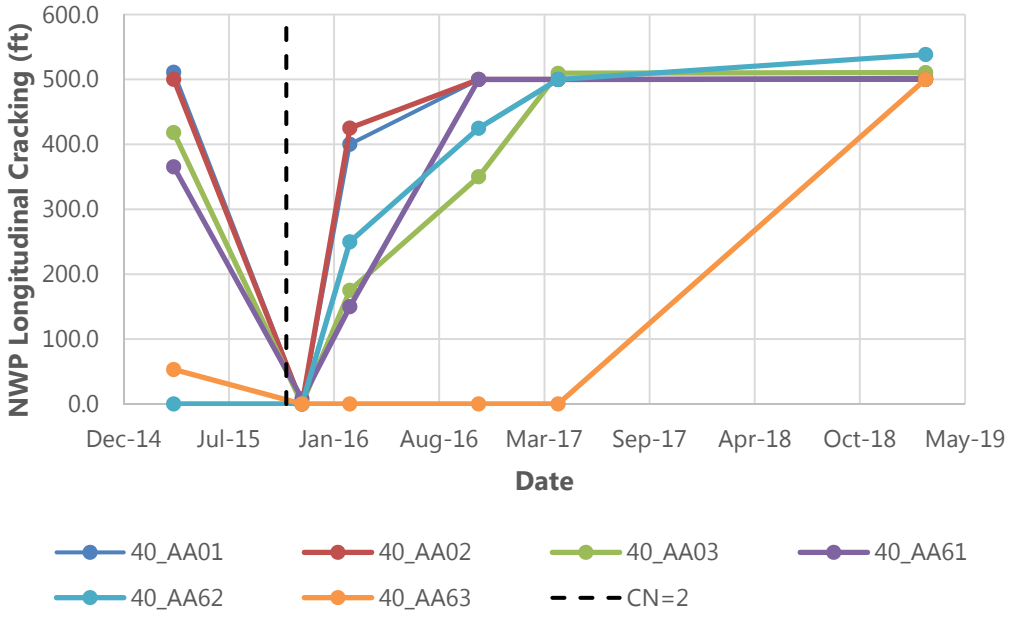


**Figure 10. Time history of the length of NWP longitudinal cracks. Most of the NWP longitudinal after the overlay placed in CN=2 are associated with the between lane longitudinal joint created during the construction process.**

Another aspect of overlays that creates NWP longitudinal cracks is the construction sequence for mill and overlay test sections on roads with two lanes in the same direction of traffic. Because of traffic control issues, the construction sequence must require single lane closures while milling and overlays procedures were performed in each lane. This type of construction sequence creates cold longitudinal joint between lanes since the new asphalt layer is placed at different time. These joints have issues with adequate compaction of material directly adjacent to the joint. This type of mechanism would explain the rapid rise in NWP longitudinal cracking on all the test sections after overlay. The apparent exception appears to be section 63.

Figure 11 is an image of section 63 in 2016 at station 0+00. The two interesting features from this image is that the left (passing) lane has an obvious different type of surface material than the experimental test section in the right lane. The longitudinal construction joint between the right and left lane was not rated

as an NWP longitudinal crack. (Note the open graded texture of this Stone Matrix Mixture is what allows the ability to put more asphalt into the mix.) .

**Figure 11. Image of section 40_AA63 in 2016 showing the new as-placed SMA mixture in the right lane. Note the tight center-lane longitudinal joint and different surface type uses in the left lane.**

Figure 12 is an image of the same portion of the test section in 2019, where the between lane longitudinal construction joint is now rated as a full test section length NWP longitudinal crack. From this visual evidence it appears that the NWP longitudinal cracking variability shown in figure 10 appears to be related to how the between lane longitudinal joint is rated in the distress surveys.

**Figure 12. Image of section 40_AA63 in 2019, when the between lane longitudinal joint is now rated as a full test section length NWP longitudinal crack.**

The overall observation from this analysis is that the rise in NWP longitudinal cracking shown in figure 10 is more likely due to degradation of the between lane longitudinal joint created during overlay placement, than a reflection cracking mechanism.

## Transverse Cracking

Figures 13 and 14 show the total number and total length of transverse cracks observed on the six test sections prior to and following the application of the AC overlay in 2015. As shown in the figures, transverse cracking varied by section prior to the overlay with section 40_AA03 exhibiting the most cracking, 123 total transverse cracks or 841.6 ft of cracking, and section 40_AA62 exhibiting the least cracking, with 0 transverse cracks in 2015.

While the transverse cracking reported prior to the AC overlay varied from section to section, no transverse cracking was observed on any of the sections until April 2017 when one transverse crack, 2.3 ft in length, was observed on section 40_AA01, and 49 transverse cracks, 136.1 feet in total length, were observed on section 40_AA61. By March of 2019, transverse cracking was also observed on sections 40_AA02 and 40_AA03. The transverse cracking observed in 2019 ranged between 320.9 ft (49 total cracks) on test section 40_AA02 and 730.4 ft (178 total cracks) on section 40_AA61.

It appears that transverse cracking observed following the application of the overlay is related to the amount of transverse cracking observed prior to the overlay. As shown in Figures 13 and 14, the only sections where transverse cracking was not observed following the AC overlay are the sections that had little to no transverse cracking prior to the overlay (sections 40_AA62 and 40_AA63). A shown in the image in Figure 8 of test section 40_AA61, the pre-overlay cracking was rated as block cracking. As can be seen in Figure 8, many of the "blocks" had significant transverse cracks although they were not rated as transverse cracks. Figure 15 is a pre-overlay image of test section 40_AA62 showing very similar cracking patterns to those on test section 40_AA62. For sections that did have transverse cracking following the AC overlay, transverse cracking reappeared between 17 and 40 months following the overlay event. There is some indication that the transverse cracking observed following the overlay is a reflection of transverse cracking observed prior to the overlay.

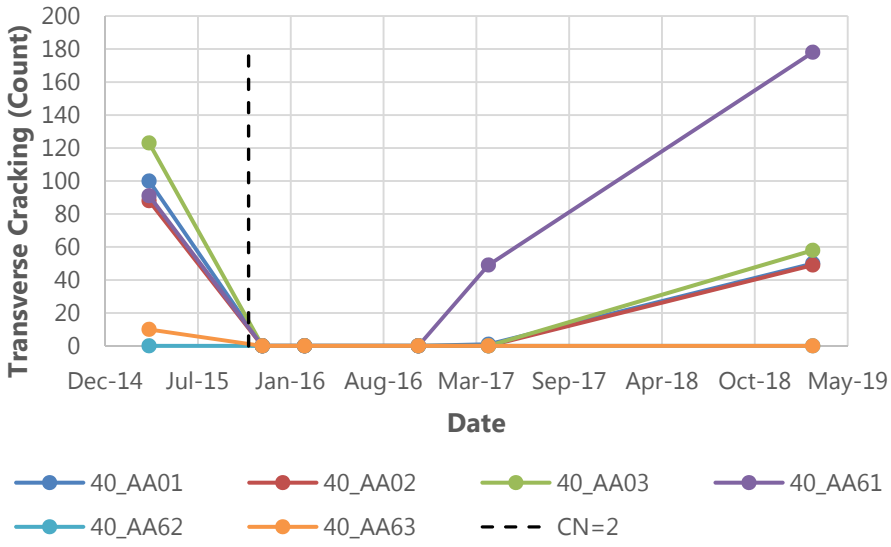


**Figure 13. Time history of the number of transverse cracks.**

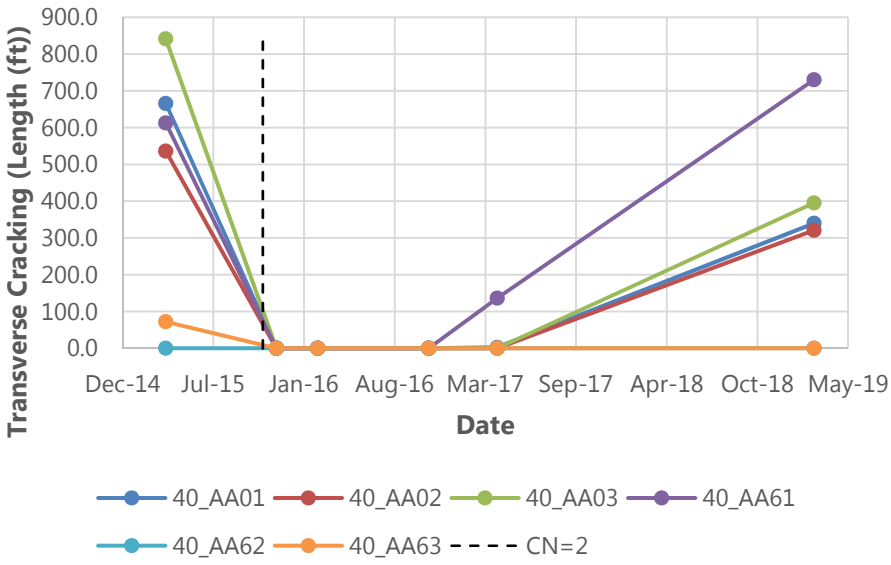


**Figure 14. Time history of the total length of transverse cracks.**

**Figure 15. Preoverlay image of section 40_AA61. This section has a similar cracking pattern to section 40_AA62, shown in figure 8 that were rated as block cracking. The transverse cracks on this test section were rated as transverse cracks.**

Because pavement distresses have only been monitored over a three-year period after application of the AC overlay, it is important to continue to monitor transverse cracking on the test sections. By doing so, the initiation of cracking and the effect of the extent of cracking prior to application of the overlay on the propagation of cracking following the overlay can be better studied.

**Figure 16. Image of Section 40_AA62 in March 2019. This is an image of the same portion of test section as shown in figure 15. The location and pattern of the cracks support the reflection cracking hypothesis. This test section had the highest amount of post-overlay transverse cracking in 2019.**

## Edge Cracking

Edge cracking is defined by LTPP as crescent-shaped or fairly continuous cracks that intersect the outside edge of a pavement that has unpaved shoulders. Longitudinal cracks within 2 feet of the outside lane edge are also classified as edge cracks. Figure 17 summarizes the total length of edge cracking that was observed prior to and after the application of the AC overlay in November 2015. Edge cracking prior to the overlay was the same for all six sections; each section had 500 ft of edge cracking, which is the full length of the test sections. Figures 8 and 15 provide an example of what was rated as full test-section length edge cracking. A relatively small longitudinal crack at the edge of the fog line, or outside lane edge stripe, is what was being rated as full test-section-length edge cracking. Following the overlay, edge cracking began to be observed four months after the application of the AC overlay for sections 40_AA01, 40_AA02, 40_AA61, and 40_AA62 with edge cracking ranging from 14.4 feet for section 40_AA02 and 227.3 feet for test section 40_AA61 in March 2016. By March 2019, five of the six test sections had edge cracking ranging from 86.3 ft for section 40_AA62 and 470.2 ft for section 40_AA01. Test section 40_AA03 was the only section where edge cracking did not reappear by March 2019 following the overlay.

The edge cracking mechanism is typically associated with loss of edge support on pavements with unpaved shoulders. Edge cracking can also be influenced cracks in the paint lines at the outside pavement edge. Few conclusions can be drawn about the effect of the type or thickness of asphalt overlay on the amount of edge cracking observed following the application of the overlay.

## Block Cracking

Block cracking was observed on three sections prior to the application of the overlay on April 2015 – 1,168.50 $ft^2$, 3,628.30 $ft^2$, and 3,525.00 $ft^2$ for sections 40_AA61, 40_AA62, and 40_AA63, respectively. No block cracking has been observed since the application of the overlay. As previously noted block cracking is a combination of longitudinal and transverse cracks which can confound the interpretation

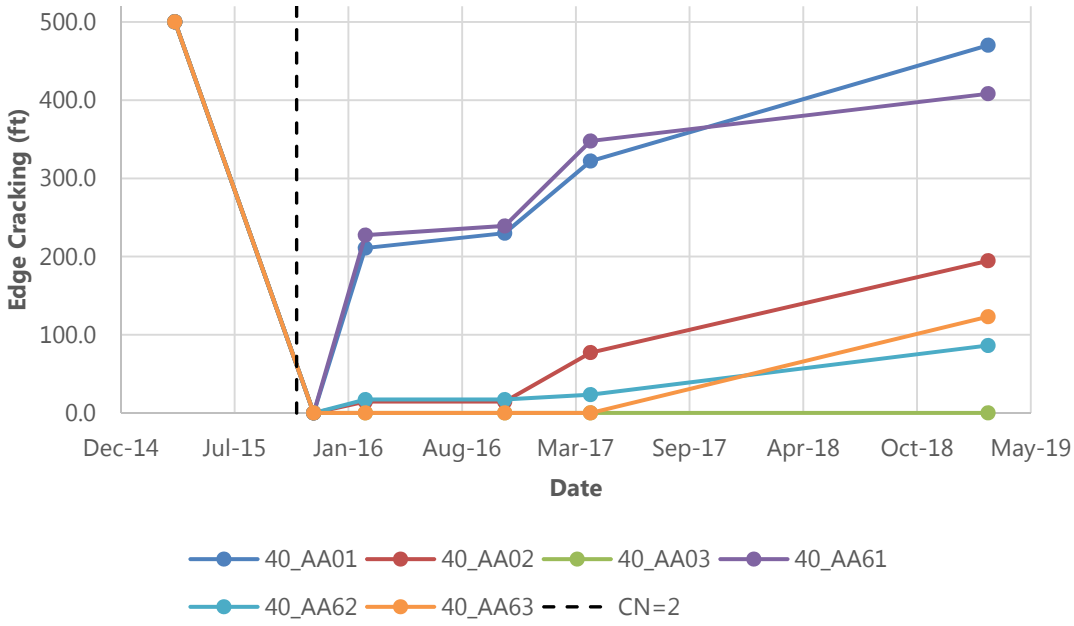


**Figure 17. Time history of the total length of edge cracking.**

## IRI

The IRI observed for the test sections over time is shown in Figure 18. Prior to the application of the AC overlay, the measured IRI values on the test sections ranged from 67.4 in/mi (excellent condition) on section 40_AA03 to 141.7 in/mi (very poor condition) on section 40_AA62. Following the application of the overlay, there was a significant decrease in the IRI of the test sections, with values in 2015 (after overlay) ranging between 38 and 60 in/mile. The IRI in 2016 remained low with values ranging from 40.6 in/mi (section 40_AA02) to 57.3 in/mi (section 40_AA63), but slowly increased to values ranging from 43.3 in/mi (section 40_AA03) to 78.4 in/mi (section 40_AA63) in 2019.

## Rutting

The measured rutting (average of maximum rut depth measurements on left and right sides of lane using 6-foot straightedge) over time for the sections is shown in Figure 19. Prior to the application of the AC overlay, the rutting values observed on the test sections ranged from 0.2 in (section 40_AA61) to 0.35 in (sections 40_AA62 and 40_ AA63). Following the milling and application of the AC overlay, there was a significant decrease in rutting, with values in 2016 ranging between 0.0 in (section 40_AA01) and 0.12 in (sections 40_AA62 and 40_ AA63). Rutting measured in 2016 remained consistent through 2017, with values ranging from 0.0 in (Section 40_AA01) to 0.12 in (Sections 40_AA62 and 40_ AA63) by 2017. Prior to and after application of overlay, Sections 40_AA63 and 40_AA62 reported similar rutting values.

Figure 19 also shows that rutting values decrease further with time with values below 0.15 inches by 2017. However, it must be recognized that the rutting values in question are small and the changes in question are within the device's measurement error range (± 0.08 inches).

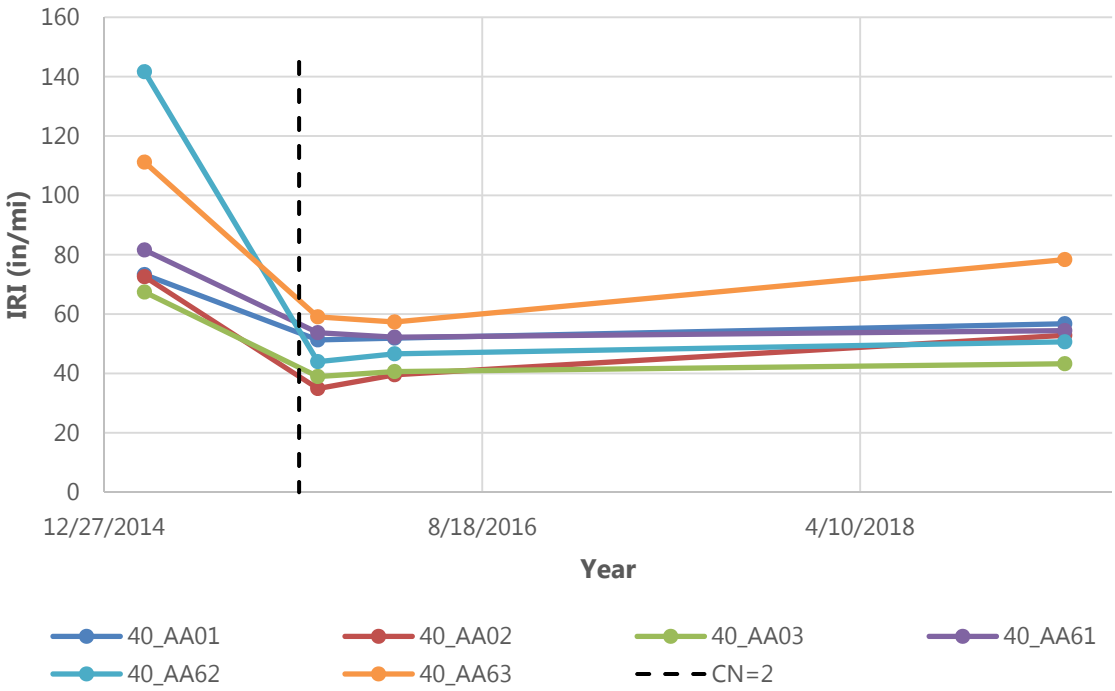


**Figure 18. Time history plot of pavement roughness.**

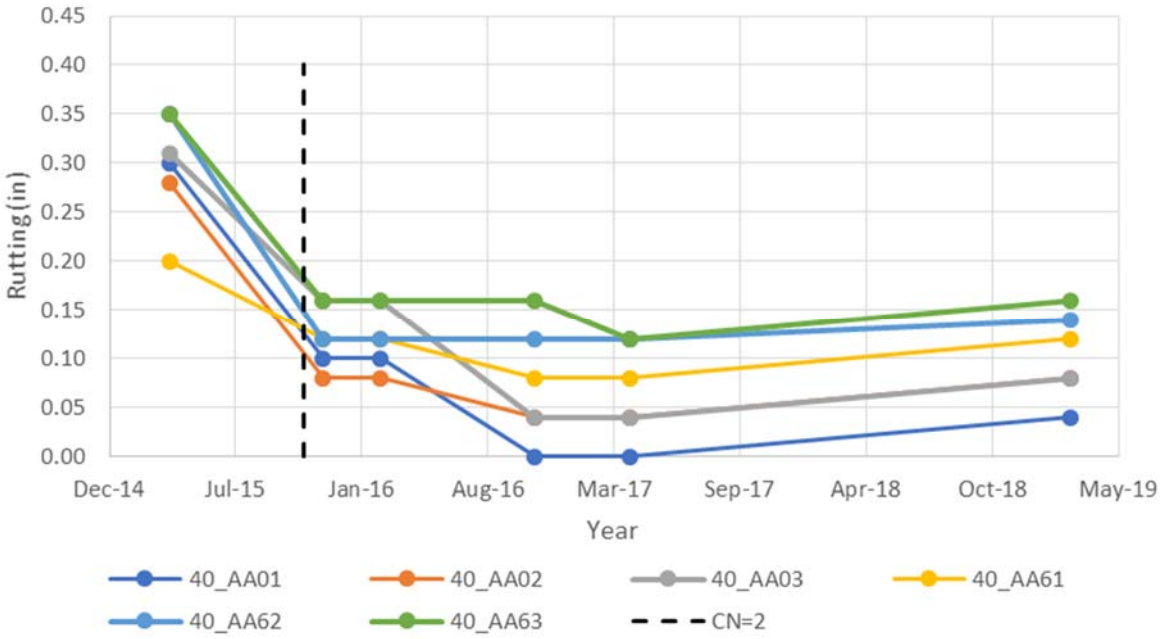


**Figure 19. Time history plot of average rut depth computations.**

## SUMMARY OF FINDINGS

In this review of information concerning the performance history of the six test sections, the following information was presented:

- The test sections were incorporated into the LTPP program in March 2015 as part of the SPS-10 Warm Mix Asphalt Experiment. Each test section was milled and received a 2 in (nominal) AC overlay in November of 2015. Section 40_AA01 received a conventional HMA overlay, sections 40_AA02, 40_AA03, 40_AA61, and 40_AA62 received WMA overlays incorporating different WMA additives, and section 40_AA63 received a SMA overlay.
- While some similar features are noted among the test sections prior to overlay, there were differences in the way similar distress features on each test section was interpreted. Block cracking, which is a combination of transverse and longitudinal cracks can confound some cracking distresses if the cracking distresses are analyzed separately.
- All pavement distresses, deflection and IRI were reduced immediately after the application of the experimental overlay, as is to be expected.
- Section 40_AA61, which had virgin asphalt one grade lower than the core experimental test sections, and a chemical WMA additive has exhibited the greatest amount of cracking in the experimental overlay. The PG binder high temperature grade is meant to address rutting issues, while the low temperature grade is meant to address cracking due to low pavement temperatures. All of the experimental sections, except the SMA test section, are reported to contain RAS. While RAS is known to stiffen the AC mixtures, so far this mix is showing the most advanced cracking post- overlay.
- The presence of NWP longitudinal cracking following the overlay at similar levels as prior to the overlay is due to the longitudinal cold joint between lanes created by the construction process being classified as a crack.
- At this point in the performance history, the HMA test section appears to have slightly better performance than the warm mix sections, but this is an intermediate observation.

Tables 5 and 6 provide a summary of the distresses observed prior to and immediately after application of the AC overlay in 2015, while Table 7 presents the most recent distress information; i.e., from the latest data collection survey.

**Table 5. Summary of distresses prior to the overlay (in 2015).**

| Section | Fatigue Cracking (sq. ft.) | NWP Longitudinal Cracking (ft) | Transverse Cracking (Count and Length) | Edge Cracking (ft) | Block Cracking (sq. ft.) | IRI (in/mi) | Rutting (in) | Deflection (mil) |
|---|---|---|---|---|---|---|---|---|
| 40_AA01 | 447.8 | 511 | 100 (665.8 ft) | 500 | 0 | 73.31 | 0.30 | 25.8 |
| 40_AA02 | 769.6 | 500.2 | 88 (536.3 ft) | 500 | 0 | 72.61 | 0.28 | 27.8 |
| 40_AA03 | 255.1 | 418.2 | 123 (841.6 ft) | 500 | 0 | 67.42 | 0.31 | 26.9 |
| 40_AA61 | 596.3 | 365.4 | 91 (612.7 ft) | 500 | 1168.50 | 81.61 | 0.2 | 22.3 |
| 40_AA62 | 2279.8 | 0 | 0 (0 ft) | 500 | 3628.30 | 141.67 | 0.35 | 28.4 |
| 40_AA63 | 1612.4 | 53.1 | 10 (72.2ft) | 500 | 3525.00 | 111.2 | 0.35 | 23.9 |

**Table 6. Summary of distresses following the overlay (in 2015)**

| Section | Fatigue Cracking (sq. ft.) | NWP Longitudinal Cracking (ft) | Transverse Cracking (Count and Length) | Edge Cracking (ft) | Block Cracking (sq. ft.) | IRI (in/mi) | Rutting (in) | Deflection (mil) |
|---|---|---|---|---|---|---|---|---|
| 40_AA01 | 0 | 0 | 0 | 0 | 0 | 51.32 | 0.1 | 15.7 |
| 40_AA02 | 0 | 0 | 0 | 0 | 0 | 34.91 | 0.08 | 17.3 |
| 40_AA03 | 0 | 0 | 0 | 0 | 0 | 38.97 | 0.16 | 19.4 |
| 40_AA61 | 0 | 7.9 | 0 | 0 | 0 | 53.73 | 0.12 | 18.8 |
| 40_AA62 | 0 | 0 | 0 | 0 | 0 | 43.97 | 0.12 | 18.1 |
| 40_AA63 | 0 | 0 | 0 | 0 | 0 | 59.05 | 0.16 | 22.2 |

**Table 7. Summary of latest distresses data (in 2019).**

| Section | Fatigue Cracking (sq. ft.) | NWP Longitudinal Cracking (ft) | Transverse Cracking (Count and Length) | Edge Cracking (ft) | Block Cracking (sq. ft.) | IRI (in/mi) | Rutting (in) (2019) | Deflection (mil) (Nov-2016) |
|---|---|---|---|---|---|---|---|---|
| 40_AA01 | 1.1 | 502.6 | 50 (339.9 ft) | 470.2 | 0 | 56.8 | 0.04 | 14.1 |
| 40_AA02 | 1.1 | 500.0 | 49 (320.9 ft) | 194.6 | 0 | 52.9 | 0.08 | 15.6 |
| 40_AA03 | 0.0 | 510.5 | 58 (395.4 ft) | 0.0 | 0 | 43.3 | 0.08 | 17.8 |
| 40_AA61 | 139.9 | 500.0 | 178 (730.4 ft) | 408.2 | 0 | 54.4 | 0.12 | 17.2 |
| 40_AA62 | 0.0 | 538.4 | 0 (0 ft) | 86.3 | 0 | 50.7 | 0.14 | 19.4 |
| 40_AA63 | 0.0 | 500.0 | 0 (0 ft) | 123.0 | 0 | 78.4 | 0.16 | 25.7 |

# FORENSIC EVALUATION RECOMMENDATIONS

It is recommended that the desktop study be extended to further investigate the various topics addressed in this technical memorandum by carrying out the following:

- Continue performance monitoring of test sections in accordance with current LTPP policy to completion of the lifecycle of the current experimental SPS-10 based overlay test sections.
- Perform FWD testing on a two-year interval to measure the change in structural capacity as subsurface pavement distresses are expected to reflect through the overlays.
- Re-perform this or an experiment wide analysis, when the results of the time history laboratory data tests are available.
- Consider use of ground penetrating radar (GPR) to more accurately characterize the thickness of the pavement layers and identification of saturated regions in the unbound base materials in each test section, and especially the top AC layers, which appear variable.

## Attachment A. Photographs of New Mexico SPS-10 test sections.

**Photograph 1. Picture of test section 40_AA01 in 2017 (Station 0+00 looking westbound).**

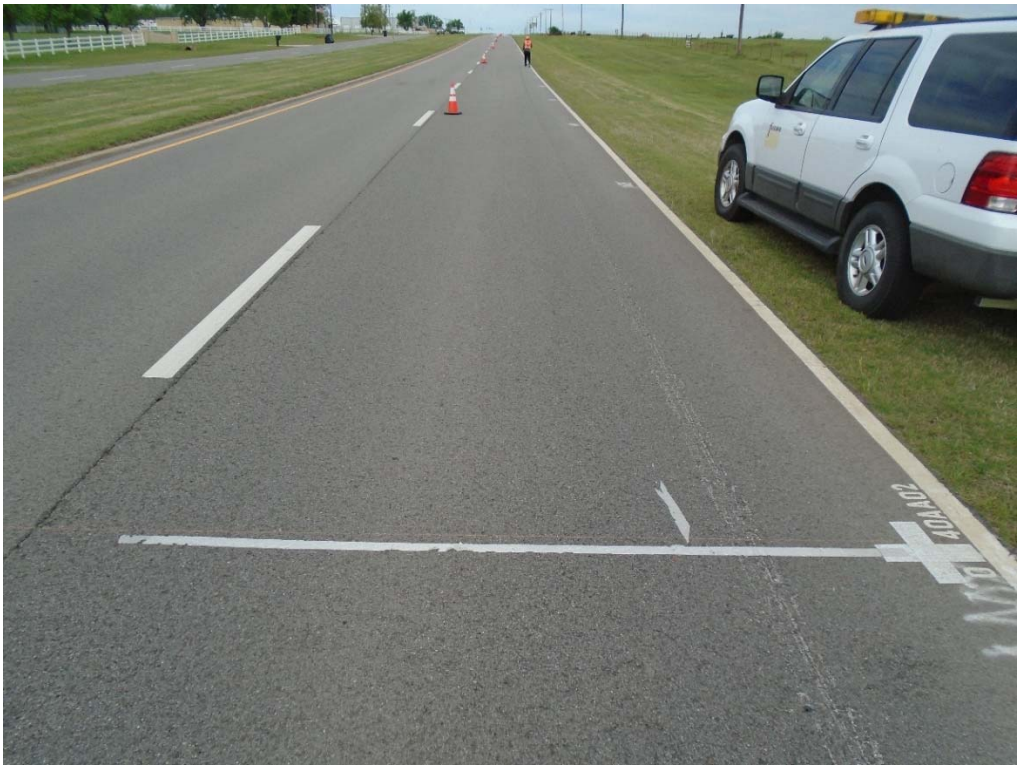


**Photograph 2. Picture of test section 40_AA02 in 2017 (Station 0+00 looking westbound).**

**Photograph 3. Picture of test section 40_AA03 in 2017 (Station 0+00 looking westbound).**

**Photograph 4. Picture of test section 40_AA61 in 2017 (Station 0+00 looking westbound).**


**Photograph 5. Picture of test section 40_AA62 in 2017 (Station 0+00 looking westbound).**


**Photograph 6. Picture of test section 40_AA63 in 2017 (Station 0+00 looking westbound).**